

An Evidential Real-Time Multi-Mode Fault Diagnosis Approach Based on Broad Learning System

Chen Li¹, Zeyi Liu¹, Limin Wang², Minyue Li³, Xiao He¹

1. Department of Automation, Tsinghua University, Beijing, China
E-mail: {yan12, liuzy21}@mails.tsinghua.edu.cn, hexiao@tsinghua.edu.cn

2. School of Mechanical and Electrical Engineering, Guangzhou University, Guangzhou, China
E-mail: wanglimin0817@163.com

3. Wujiang Laboratory, Guiyang, China
E-mail: philoinfo@gmail.com

Abstract: Fault diagnosis is a crucial area of research in the industry due to diverse operating conditions that exhibit non-Gaussian, multi-mode, and center-drift characteristics. Currently, data-driven approaches are the main focus in the field, but they pose challenges for continuous fault classification and parameter updates of fault classifiers, particularly in multiple operating modes and real-time settings. Therefore, a pressing issue is to achieve real-time multi-mode fault diagnosis for industrial systems. To address this problem, this paper proposes a novel approach that utilizes an evidence reasoning (ER) algorithm to fuse information and merge outputs from different base classifiers. These base classifiers are developed using a broad learning system (BLS) to improve good fault diagnosis performance. Moreover, in this approach, the pseudo-label learning method is employed to update model parameters in real-time. To demonstrate the effectiveness of the proposed approach, we perform experiments using the multi-mode Tennessee Eastman process dataset.

Key Words: Fault diagnosis, multi-mode, real-time, broad learning system (BLS), evidence reasoning (ER)

1 Introduction

Fault diagnosis plays a crucial role in ensuring the efficiency, stability, and reliability of industrial processes, making it a focal point in both academic research and industrial applications [1, 2]. However, with the development of integrated, scaled, and complex systems, the challenges posed by fault diagnosis in industrial processes are becoming increasingly demanding. Recent advances in computer and sensor technologies have simplified the data acquisition process and given rise to significant developments in data-driven methods for fault diagnosis [3]. Practical industrial processes often involve multiple operating modes, which give rise to non-Gaussian, multimodal, and center-drifting data features. These characteristics pose a challenge for research into fault diagnosis in industrial production [4].

Some methods have been used by scholars for multi-mode fault diagnosis tasks, including time-synchronous averaging [5], and order tracking [6], among others. Li *et al.* proposed an adaptive cost function ridge estimation (CFRE) method for extracting fault-related characteristic curves in a time-frequency representation without the need for rotational speed sensors [7]. However, the fault features extracted by these methods are only robust to speed fluctuations or white noise interference, but are sensitive to other changes in the operating environment. Su *et al.* proposed a dilated convolution deep belief network-dynamic multi-layer perceptron (DCDBN-DMLP) for recognizing bearing faults under varying operating conditions,

which uses dilated convolution deep belief network, multi-layer domain adaptation, and pseudo label technology to address distribution discrepancies between source and target domains [8]. Li *et al.* presented the Modified Auxiliary Classifier GAN (MACGAN) as a novel supervised fault diagnosis model for limited data in rotational machinery [9]. Moreover, Hanachi *et al.* proposed a hybrid diagnostic framework combining a data-driven multi-mode fault parameter estimation scheme with a fault propagation model to diagnose hidden incipient faults in gas turbine engine components [10]. However, deep learning methods depend on a large amount of feature data from different operating conditions, which is often difficult to obtain in practical engineering. As such, there is a need to develop a fault diagnosis independent of deep learning that is robust to feature data distribution and operating conditions.

In recent years, various neural network structures have emerged due to the development of neural networks. One such feedforward neural network structure is the Broad learning system (BLS), which provides generalization capability for function approximation and does not rely on depth [11]. BLS is a universal approximator for continuous functions on a tight set and is known for its fast learning properties, scaling well to different fields. BLS employs a unique incremental update strategy allowing fast updating and adaptation to new data without requiring retraining, making it highly useful in real-time fault diagnosis tasks [12, 13]. Unlike traditional neural networks, BLS's incremental update approach can address issues encountered during the training process, such as vanishing and exploding gradients. As such, BLS has extensive applications in fault diagnosis [14, 15].

This work was supported by the National Natural Science Foundation of China under grant 62163012, National Key Research and Development Program of China under grant 2022YFB25031103, and Huaneng Group Science and Technology Research Project. (*Corresponding author: Xiao He*)

In this paper, a real-time multi-mode fault diagnosis approach is proposed, which combines the BLS model with the evidence reasoning (ER) algorithm. The approach is summarized as follows:

- 1) An improved learning scheme is designed to adjust model parameters dynamically during operation, enabling effective handling of varying environmental conditions in real time.
- 2) We adopt the ER rule to combine prediction results and assign appropriate weights of evidence to ensure its suitability for various fault scenarios.
- 3) Several experiments are conducted using the datasets from the multi-mode Tennessee Eastman process. The results demonstrate its superiority for handling tasks involving real-time multi-mode fault diagnosis.

The rest of the paper is organized as follows: Section 2 provides an introduction to basic concepts. Section 3 goes into detail about the proposed approach, which includes a BLS model, evidence reasoning algorithm, and adaptive incremental update procedure based on pseudo-label learning. Section 4 describes several comparison experiments conducted based on the MMTEP dataset. In the final section, Section 5, concluding remarks are presented.

2 Preliminaries

2.1 Broad learning system

The broad learning system (BLS) is an advanced neural network structure derived from the random vector functional-link (RVFL) networks [11]. Its simple structure and exceptional computational speed make it ideal for real-time prediction tasks with limited data. Given measurement data $X \in \mathbb{R}^{n \times m}$ and label $Y \in \mathbb{R}^{n \times l}$, the following mapping scheme is utilized:

$$Z_i = \phi(XW_{e_i} + \beta_{e_i}) \in \mathbb{R}^{n \times N_e}, \quad (1)$$

where $\phi(*)$ denotes the feature mapping function, and W_{e_i} is the weight matrix of the i^{th} randomly generated feature group. Additionally, β_{e_i} is the randomly produced bias vector, and N_e is the number of feature nodes in each feature group. The final feature layer can be represented as $Z^{N_f} = [Z_1, Z_2, \dots, Z_{N_f}]$. Direct correlation exists between the random feature layer Z^{N_f} and the original data X . Further mapping operations are necessary to expand the information in X , namely, enhanced node mapping:

$$H_j = \xi(Z^{N_f}W_{h_j} + \beta_{h_j}) \in \mathbb{R}^{n \times N_g}, \quad (2)$$

where $\xi(*)$ denotes the enhanced node mapping function, W_{h_j} is the weight randomly generated for the j^{th} enhancement group, β_{h_j} is the bias vector randomly produced for the j^{th} enhancement group, and N_g is the number of enhanced nodes in each enhancement group, and the enhancement layer can be represented as: $H^{N_h} = [H_1, H_2, \dots, H_{N_h}]$.

From the calculation process, it can be seen that the enhanced nodes are obtained through the calculation of the feature layer Z^{N_f} , which indicates that the enhancement layer

H^{N_h} is correlated with the original data, and this further extracts information. Assuming $A^Z = [Z^{N_f} | H^{N_h}]$, the mapping relationship between data X and label Y can be expressed as follows:

$$\begin{aligned} Y &= A^Z W_N^M \\ &= [Z^{N_f} | H^{N_h}] W_N^M \\ &= [Z_1, Z_2, \dots, Z_{N_f} | H_1, H_2, \dots, H_{N_h}] W_N^M. \end{aligned} \quad (3)$$

2.2 Evidence reasoning algorithm

The ER algorithm offers a method for logically combining various sources of information, even when faced with uncertainty and inconsistency [16, 17]. This approach can be adapted to different decision-making tasks and is particularly useful in diagnosing faults involving multiple classifiers.

Define the framework of discernment (FOD) as follow:

$$F = \{F_0, F_1, F_2, \dots, F_N\}, \quad (4)$$

where F_i represents the i^{th} levels of assessment. All inputs transformed into confidence distribution form can be integrated through the ER fusion framework to obtain the levels of assessment, expressed in distribution form as follows:

$$O(F) = \{(F_n, \beta_n), n = 0, 1, \dots, N\}, \quad (5)$$

where O represents a conversion model that transforms FOD F into confidence distribution. β_n can be calculated through the ER algorithm, and its form can be summarized as follows:

Firstly, the relative weights and degrees of belief are combined to convert the degrees of belief into basic probability masses using the following equations:

$$m_{n,i} = w_i \beta_{n,i}(x), n = 0, 1, \dots, N; i = 1, \dots, L, \quad (6)$$

$$m_{F,i} = 1 - \sum_{n=1}^N m_{n,i} = 1 \quad (7)$$

$$- w_i \sum_{n=1}^N \beta_{n,i}(x), i = 1, \dots, L,$$

$$\bar{m}_{F,i} = 1 - w_i, i = 1, \dots, L, \quad (8)$$

$$\tilde{m}_{F,i} = w_i \left(1 - \sum_{n=1}^N \beta_{n,i}(x) \right), i = 1, \dots, L, \quad (9)$$

where $m_{F,i} = \bar{m}_{F,i} + \tilde{m}_{F,i}$ and $\sum_{i=1}^L w_i = 1$. $m_{n,i}$ is the basic probability mass of x when the result of assessment is considered to be F_n . w_i is the relative weights coefficient of the evidence i . $m_{F,i}$ is the probability mass not currently assigned to any single level of assessment and can be split into two parts: $\bar{m}_{F,i}$ and $\tilde{m}_{F,i}$. The ER algorithm is used to merge the basic probability masses.

$$m_{n,I(i+1)} = u_{i+1} [m_{n,I(i)} m_{n,i+1} + m_{n,I(i)} m_{F,i+1} + m_{F,I(i)} m_{n,i+1}], \quad (10)$$

$$m_{F,I(i)} = \bar{m}_{F,I(i)} + \tilde{m}_{F,I(i)}, \quad (11)$$

$$\begin{aligned} \tilde{m}_{F,I(i+1)} = & u_{i+1} [\tilde{m}_{F,I(i)} \tilde{m}_{F,i+1} \\ & + \tilde{m}_{F,I(i)} \bar{m}_{F,i+1} + \bar{m}_{F,I(i)} \tilde{m}_{F,i+1}], \end{aligned} \quad (12)$$

$$\bar{m}_{F,I(i+1)} = u_{i+1} [\bar{m}_{F,I(i)} \bar{m}_{F,i+1}], \quad (13)$$

$$u_{i+1} = \left[1 - \sum_{n=1}^N \sum_{\substack{t=1 \\ t \neq n}}^N m_{n,I(i)} m_{t,i+1} \right]^{-1}, \quad (14)$$

$$\beta_n = \frac{m_{n,I(L)}}{1 - \bar{m}_{F,I(L)}}. \quad (15)$$

3 The Proposed Approach

In this section, we propose a model based on BLS and ER algorithm. The model is akin to ensemble learning in which information fusion techniques are used to combine the results of multiple classifiers to improve the accuracy of a prediction. Additionally, the model parameters are updated incrementally based on dynamic data streams to increase the adaptability of the model.

A multi-mode fault diagnosis model that fuses the results of multiple classifiers across various operating conditions is proposed for the task of fault diagnosis. An ensemble method combines several complementary classifiers, leveraging their individual strengths and weaknesses to improve the overall accuracy of fault diagnosis. This approach allows for the model to perform with high precision and efficiency, making it a valuable tool for industrial applications in complex and dynamic environments.

The modeling process for a given classifier C_k based on BLS can be described as follows:

$$z_{i,k} = \phi(XW_{e_{i,k}} + \beta_{e_{i,k}}), \quad (16)$$

Let $z^{N_f} = [z_{1,k}, z_{2,k}, \dots, z_{N_f,k}]$. After completing one iteration of the random weight vector mapping, it is advantageous to conduct another iteration to refine the classifier and gain additional knowledge from the input data. Through this iterative process, the classifier can become more accurate and robust to sources of noise or variability in the data.

$$h_{j,k} = \xi(z^{N_f} W_{h_{j,k}} + \beta_{h_{j,k}}), \quad (17)$$

Denote $h^{N_h} = [h_{1,k}, h_{2,k}, \dots, h_{N_h,k}]$. Similar to the process of computing the pseudo-inverse using BLS, it is necessary to flatten and combine the results of two rounds of random mappings $A_{p,k} = [z_k^{N_f} | h_k^{N_h}]$. The weight parameters of classifier C_k can be obtained as follows:

$$W_{N,k}^M = A_{p,k}^\dagger Y \quad (18)$$

The prediction for the data stream $x(t)$ at t time can be calculated based on Eqs. (16)-(18) as:

$$\hat{Y}_k(t) = A_k(t) W_{N,k}^M = [\hat{y}_{1,k}(t), \hat{y}_{2,k}(t), \dots, \hat{y}_{N,k}(t)] \quad (19)$$

After modeling K classifiers, the fusion process of their prediction results at t time based on the ER algorithm is as follows:

$$m_{n,k} = w_{n,k} \hat{y}_{n,k}(t), n = 0, 1, \dots, N; k = 1, \dots, K, \quad (20)$$

$$m_{n,k}^F = 1 - \sum_{n=1}^N m_{n,k} \quad (21)$$

$$= 1 - w_{n,k} \sum_{n=1}^N \hat{y}_{n,k}(t), k = 1, \dots, K,$$

$$\bar{m}_{n,k}^F = 1 - w_{n,k}, n = 0, 1, \dots, N; k = 1, \dots, K, \quad (22)$$

$$\tilde{m}_{n,k}^F = w_{n,k} \left(1 - \sum_{n=1}^N \hat{y}_{n,k}(t) \right), \quad (23)$$

$$n = 0, 1, \dots, N; k = 1, \dots, K,$$

$$m_{n,I(k+1)} = u_{k+1} [m_{n,I(k)} m_{n,k+1} + m_{n,I(k)} m_{n,k+1}^F + m_{n,I(k)}^F m_{n,k+1}], \quad (24)$$

$$m_{n,I(k)}^F = \bar{m}_{n,I(k)}^F + \tilde{m}_{n,I(k)}^F, \quad (25)$$

$$\begin{aligned} \tilde{m}_{n,I(k+1)}^F = & u_{k+1} [\tilde{m}_{n,I(k)}^F \tilde{m}_{n,k+1}^F \\ & + \tilde{m}_{n,I(k)}^F \bar{m}_{n,k+1}^F + \bar{m}_{n,I(k)}^F \tilde{m}_{n,k+1}^F], \end{aligned} \quad (26)$$

$$\bar{m}_{n,I(k+1)}^F = u_{k+1} [\bar{m}_{n,I(k)}^F \bar{m}_{n,k+1}^F], \quad (27)$$

$$u_{k+1} = \left[1 - \sum_{n=1}^N \sum_{\substack{t=1 \\ t \neq n}}^N m_{n,I(k)} m_{t,k+1} \right]^{-1}, \quad (28)$$

$$\hat{y}_{n,k}^e(t) = \frac{m_{n,I(K)}}{1 - \bar{m}_{n,I(K)}}. \quad (29)$$

The results of the prediction after fusion using the ER algorithm can be obtained as $\hat{Y}_k^e(t) = [\hat{y}_{1,k}^e(t), \hat{y}_{2,k}^e(t), \dots, \hat{y}_{N,k}^e(t)]$. Note that any classifier C_k has a corresponding relative weight $w_{n,k}$ in each system state k . $m_{n,I(1)}^F = m_{n,1}^F, n = 1, 2, \dots, N$.

In actual industrial systems, the working environment is not static, so how to adapt to environmental changes is a challenge for fault diagnosis tasks [18, 19]. The pseudo-label learning technique is a semi-supervised learning tool that utilizes both labeled and unlabeled data in a supervised manner [20]. With respect to the unlabeled data, PL selects the class with the highest predicted possibility during each weight update, treating this class as if it were the true label. In most cases, this method is compatible with almost any neural network model or training methodology. As for the new incoming data $x(t)$ at time t , we can obtain a specific output.

$$z_{i,k}(t) = \phi(x(t) W_{e_{i,k}} + \beta_{e_{i,k}}), \quad (30)$$

$$h_{j,k}(t) = \xi(z^{N_f}(t) W_{h_{j,k}} + \beta_{h_{j,k}}), \quad (31)$$

$$A_k(t) = [z_k^{N_f}(t) | h_k^{N_h}(t)]. \quad (32)$$

where $z^{N_f}(t) = [z_{1,k}(t), z_{2,k}(t), \dots, z_{N_f,k}(t)]$ and $h^{N_h}(t) = [h_{1,k}(t), h_{2,k}(t), \dots, h_{N_h,k}(t)]$. Let $A_{k,l} = A_{p,k}$. Therefore, the extended matrix can be obtained as:

$$A_{k,l+1} = \begin{bmatrix} A_{k,l} \\ A_k(t) \end{bmatrix}. \quad (33)$$

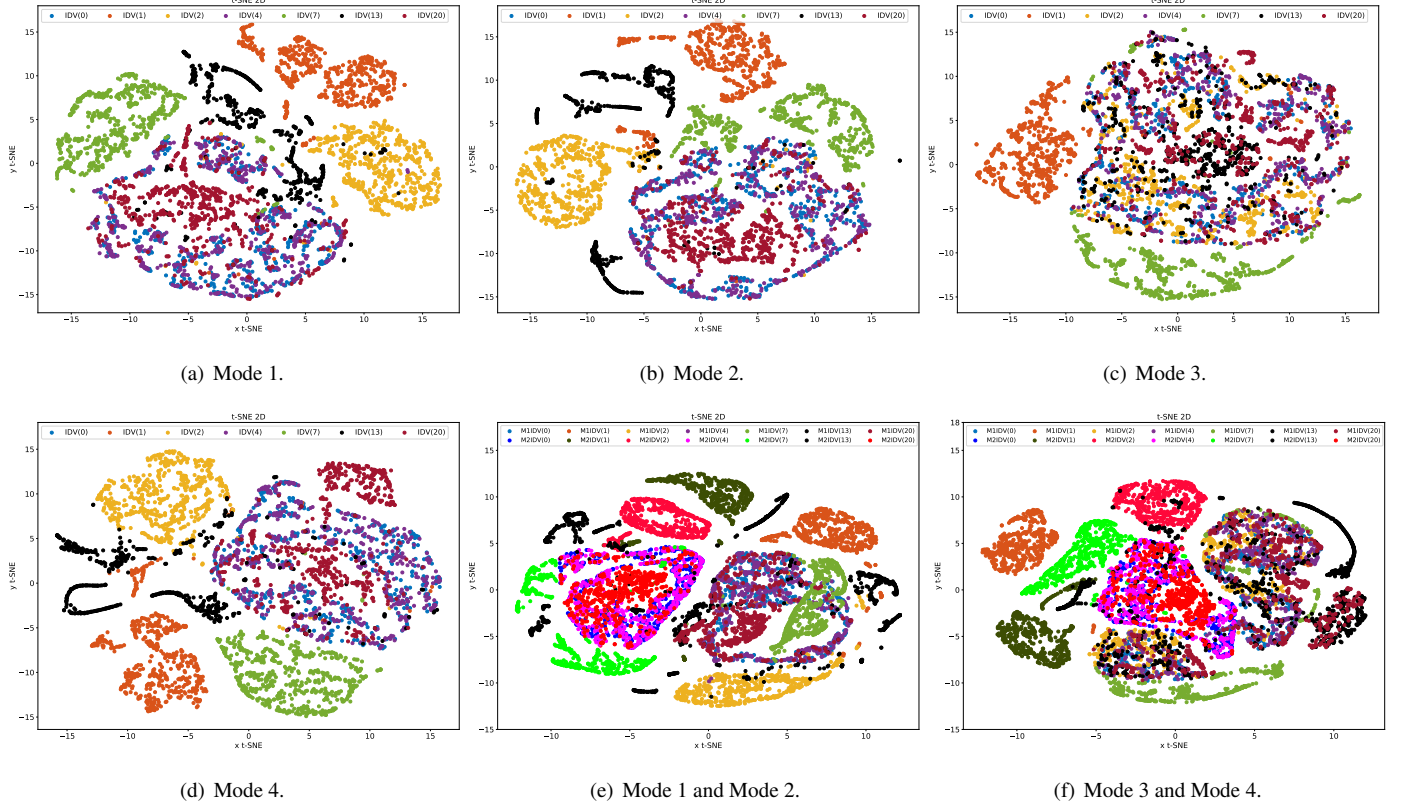


Fig. 1: The t-SNE visualization results of six faults in different modes.

Next, the related pseudo-inverse update algorithm can be derived:

$$A_{k,l+1}^\dagger = [A_{k,l}^\dagger - B_k D_k^T | B_k] \quad (34)$$

where $D_k^T = A_k(t) A_{k,l}^\dagger$,

$$B_k^T = \begin{cases} C_k^\dagger, & \text{if } C_k \neq 0, \\ (1 + D_k^T D_k)^{-1} A_{k,l}^\dagger D_k, & \text{if } C_k = 0, \end{cases} \quad (35)$$

$$C_k = A_k(t) - D_k^T A_{k,l} \quad (36)$$

The weight update after the data $x(t)$ is inputted is:

$$W_{k,l+1} = W_{k,l} + (Y_k(t) - A_k(t)W_{k,l})B_k \quad (37)$$

where $Y_k(t)$ is the true label of the new data $x(t)$. However, in practice, it is impossible to obtain the true label in real-time. Therefore, pseudo-labels generated from the model's predictive results are used to update the weights:

$$W_{k,l+1} = W_{k,l} + (\tilde{Y}_k(t) - A_k(t)W_{k,l})B_k \quad (38)$$

where $\tilde{Y}_k(t) = [\tilde{y}_{1,k}(t), \tilde{y}_{2,k}(t), \dots, \tilde{y}_{N,k}(t)]$ is the pseudo-label generated from the model's predictive results. The way

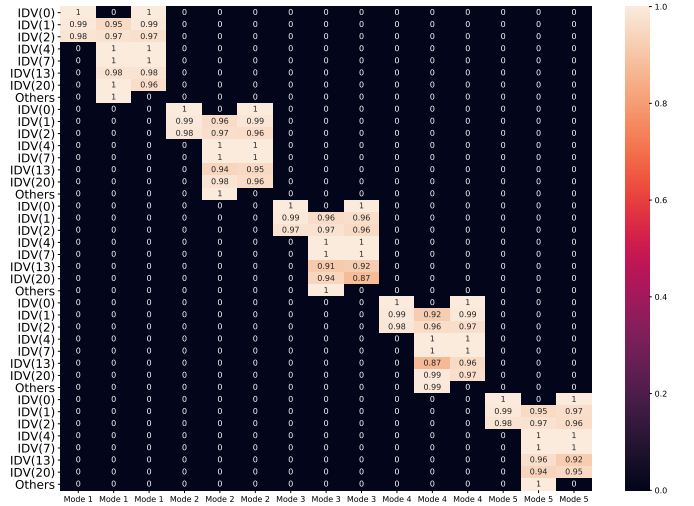


Fig. 2: The weights of base classifiers in different states of each mode.

of pseudo-label learning can be summarized as:

$$\tilde{y}_{i,k}(t) = \begin{cases} 1, & \text{if } i = \arg \max_i \hat{Y}_k^e(t), \\ 0, & \text{otherwise,} \end{cases} \quad (39)$$

For unlabelled data, pseudo-labels only pick the class with the highest predicted probability at each weight update and uti-

lize them as if they were true labels.

4 Experiments

4.1 Datasets

This study uses the multi-mode Tennessee Eastman process (MMTEP) dataset to perform experiments. The MMTEP dataset is distinct from traditional datasets as it contains multiple modalities, making it more complex and diverse. Its data streams from various sensors, such as pressure, temperature, and flow sensors, provide different modalities (e.g., bias, lag, etc.). It is based on the Tennessee Eastman process (TEP) dataset and provides an excellent resource for researching multi-mode data analysis and pattern recognition. These sensors collect data from different locations, providing various perspectives on process monitoring and control. The MMTEP dataset is applicable for various research directions, including multi-mode data analysis, multi-mode pattern recognition, and multi-mode fusion¹.

Furthermore, the MMTEP dataset provides an experimental dataset for applications such as process monitoring, fault diagnosis, and state estimation in the engineering field. These practical applications contribute to solving real-world engineering problems. There are 41 measured variables, i.e., XMEAS (1–41), and 12 manipulated variables, i.e., XMV (1–12) in MMTEP. And there are 28 faults IDV(1)-(28) and a normal state IDV(0) in dataset. Six faults in four modes, including IDV(1), IDV(2), IDV(4), IDV(7), IDV(13) and IDV(20), are selected as the experimental dataset in this paper. The visualization results of the experimental dataset are shown in Fig. 1.

4.2 Analysis of experimental results

To address the various types of faults encountered in the experiment, a specific approach is utilized in the experiment. For each mode, we randomly selected six types of fault data from the full set of faults to construct the training set. The remaining data were allocated to the test set.

To further enhance the classification accuracy, three base classifiers based on BLS were trained to achieve classification. The base classifiers were used to accurately differentiate each state in the current mode from other states (including those from other modes), allowing for a more comprehensive evaluation of the model's ability to classify. The ER algorithm is used to combine the outputs of the multiple base classifiers, resulting in improved classification accuracy. In addition, the adaptive incremental learning design was used to dynamically adjust the parameters of base classifiers with continuous updates to facilitate the response to new data streams. Fig. 2 displays the weight of each base classifier for each fault in each mode in the experiment. The results of the prediction are shown in Fig. 3.

In order to verify the effectiveness of the proposed approach, two BLS-based model training schemes were compared:

- *Scheme 1*: Train a single classifier using a training dataset containing all modes' data.
- *Scheme 2*: Train a classifier for each mode using the data from each mode separately.

The model's classification accuracy can be found in Table 1. The table displays that the model has excellent diagnostic performance in all modalities. It suggests that the combination of wide learning and evidence inference rules can effectively improve the accuracy and robustness of fault diagnosis. The approach can reduce mutual interference between modalities, thus better ensuring the accuracy and reliability of fault diagnosis.

5 Conclusion

In this study, we have proposed an enhanced model for real-time fault diagnosis in multi-mode processes. To incrementally update basic classifiers' parameters, we employ a pseudo-label learning method. This model exhibits superior performance in fault diagnosis, particularly in situations where multiple operating modes exist. Combining the BLS and ER algorithms provides more precise and consistent diagnostic outputs that are less vulnerable to interference between different operating modes. Additionally, the pseudo-label learning method improves the model's learning efficiency with fewer labeled data. We have verified the enhanced model's effectiveness using the multi-mode Tennessee Eastman Process dataset.

References

- [1] F. Liu, H. Tang, Y. Qin, C. Duan, J. Luo, H. Pu, Review on fault diagnosis of unmanned underwater vehicles, *Ocean Engineering*, 243: 110290, 2022.
- [2] W. Li, R. Huang, J. Li, Y. Liao, Z. Chen, G. He, R. Yan, K. Gryllias, A perspective survey on deep transfer learning for fault diagnosis in industrial scenarios: Theories, applications and challenges, *Mechanical Systems and Signal Processing*, 167: 108487, 2022.
- [3] Z. Liu, J. Zhang, X. He, Q. Zhang, G. Sun, D. Zhou, Fault diagnosis of rotating machinery with limited expert interaction: A multi-criteria active learning approach based on broad learning system, *IEEE Transactions on Control Systems Technology*, 2022.
- [4] K. Peng, K. Zhang, B. You, J. Dong, Quality-related prediction and monitoring of multi-mode processes using multiple PLS with application to an industrial hot strip mill, *Neurocomputing*, 168: 1094-1103, 2015.
- [5] S. Braun, The synchronous (time domain) average revisited, *Mechanical Systems and Signal Processing*, 25(4): 1087-1102, 2011.
- [6] G. He, K. Ding, W. Li, X. Jiao, A novel order tracking method for wind turbine planetary gearbox vibration analysis based on discrete spectrum correction technique, *Renewable Energy*, 87: 364-375, 2016.
- [7] Y. Li, Y. Yang, S. S. Afshari, X. Liang, Z. Chen, Adaptive cost function ridge estimation for rolling bearing fault diagnosis under variable speed conditions, *IEEE Transactions on Instrumentation and Measurement*, 71: 1-12, 2022.
- [8] H. Su, X. Yang, L. Xiang, A. Hu, Y. Xu, A novel method based on deep transfer unsupervised learning network for bearing fault diagnosis under variable working condition of unequal quantity, *Knowledge-based Systems*, 242: 108381, 2022.

¹The dataset is released at <https://github.com/THUFDD/Multi-mode-Fault-Diagnosis-Datasets-with-TE-process>

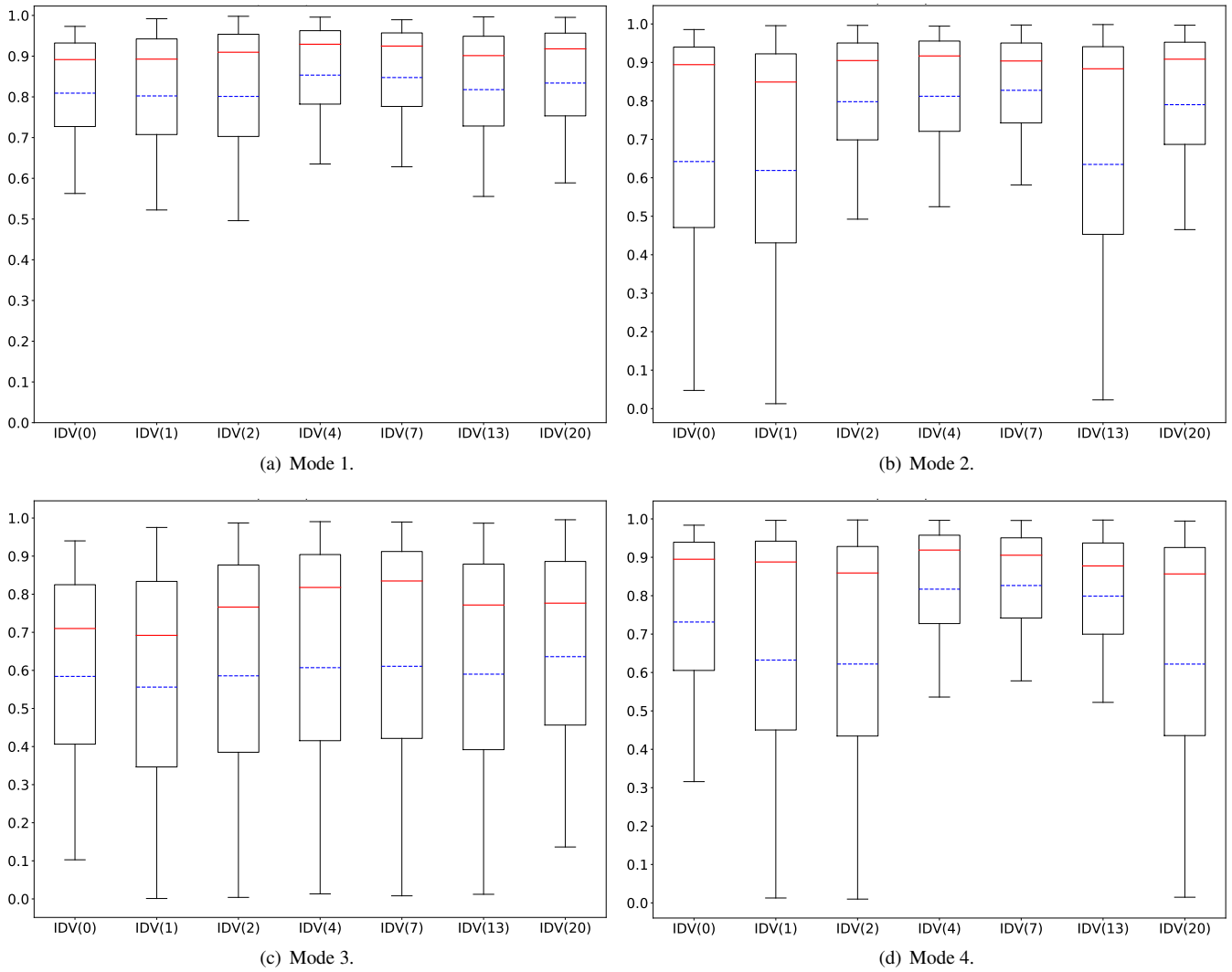


Fig. 3: The results of the prediction in different modes.

Table 1: Accuracy of different diagnostic schemes (%)

Fault	Our Scheme				Scheme 1				Scheme 2			
	Mode 1	Mode 2	Mode 3	Mode 4	Mode 1	Mode 2	Mode 3	Mode 4	Mode 1	Mode 2	Mode 3	Mode 4
IDV(0)	100	99.9	95.2	99.9	100	100	100	100	100	100	100	100
IDV(1)	100	99.8	86.7	99.9	100	100	100	100	100	100	100	100
IDV(2)	100	100	96.6	99.7	100	100	100	100	100	100	100	100
IDV(4)	100	100	99.7	100	100	85.7	0	98.4	100	100	100	100
IDV(7)	100	100	99.6	100	100	100	100	100	100	100	100	100
IDV(13)	100	99.7	90.6	100	92.9	82.1	0	100	100	100	35.4	100
IDV(20)	100	100	94.8	99.7	84.3	69.1	38.3	64.6	98	91.5	39.3	85.4

- [9] W. Li, X. Zhong, H. Shao, B. Cai, X. Yang, Multi-mode data augmentation and fault diagnosis of rotating machinery using modified ACGAN designed with new framework, *Advanced Engineering Informatics*, 52: 101552, 2022.
- [10] H. Hanachi, J. Liu, I. Y. Kim, C. K. Mechefske, Hybrid sequential fault estimation for multi-mode diagnosis of gas turbine engines, *Mechanical Systems and Signal Processing*, 115: 255-268, 2019.
- [11] C. L. P. Chen, Z. Liu, Broad learning system: An effective and efficient incremental learning system without the need for deep architecture, *IEEE Transactions on Neural Networks and Learning Systems*, vol. 29, no. 1, pp. 10-24, 2017.
- [12] X. Gong, T. Zhang, C. L. P. Chen, Z. Liu, Research review for broad learning system: Algorithms, theory, and applications, *IEEE Transactions on Cybernetics*, 2021.
- [13] Z. Liu, X. He, Real-Time Safety Assessment for Dynamic Systems With Limited Memory and Annotations, *IEEE Transactions on Intelligent Transportation Systems*, 2023.
- [14] H. Zhao, J. Zheng, J. Xu, W. Deng, Fault diagnosis method based on principal component analysis and broad learning system, *IEEE Access*, 7: 99263-99272, 2019.
- [15] Y. Fu, H. Cao, X. Chen, Adaptive broad learning system for high-efficiency fault diagnosis of rotating machinery, *IEEE Transactions on Instrumentation and Measurement*, 70: 1-11, 2021.
- [16] Y. M. Wang, J. B. Yang, D. L. Xu, Environmental impact assessment using the evidential reasoning approach, *European Journal of Operational Research*, 174(3): 1885-1913, 2006.
- [17] Z. Liu, X. He, Y. Deng, Network-based Evidential Three-way Theoretic Model for Large-scale Group Decision Analysis, *Information Sciences*, 547: 689-709, 2021.
- [18] Z. Liu, Y. Zhang, Z. Ding, X. He, An Online Active Broad Learning Approach for Real-Time Safety Assessment of Dynamic Systems in Nonstationary Environments, *IEEE Transactions on Neural Networks and Learning Systems*, 2022.
- [19] Z. Liu, Y. Deng, Y. Zhang, Z. Ding, X. He, Safety assessment of dynamic systems: An evidential group interaction-based fusion design, *IEEE Transactions on Instrumentation and Measurement*, 70: 1-14, 2021.
- [20] D. H. Lee, Pseudo-label: The simple and efficient semi-supervised learning method for deep neural networks, *Workshop on Challenges in Representation Learning, ICML*, 3(2): 896, 2013.